

Study of Silicon Photomultipliers for Positron Emission Tomography (PET) Application

Eric Oberla

5 June 2009

Abstract

A relatively new photodetector, the silicon photomultiplier (SiPM), is well suited for PET applications. It has similar sensitivity and gain to the industry standard photomultiplier tube (PMT), but has advantages such as smaller size and insensitivity to magnetic field. These properties make this detector an active area of research in the PET field. I will study a simplified setup, comprised of two antiparallel SiPM/LSO coupled detectors using a Na-22 positron source. The coincidence timing and energy resolution is determined using two methods, a CAMAC system and a fast oscilloscope. The best coincidence time resolution, 660 ps FWHM, was obtained using the digital oscilloscope. At best, the energy resolution was found to be 16.4% FWHM. Results using two types of SiPM, 1600 and 400 pixel, are presented. Data from a GEANT4 simulation of the described setup are also shown.

Introduction

Positron Emission Tomography (PET) is a medical imaging technique that is used to observe functional processes *in vivo*. The functional process of interest is observed by introducing a chemical tracer that is metabolized by certain tissues in the body. The tracer is doped with a radioisotope that undergoes positive beta decay (positron emission). A large majority of current PET scans use fluorodeoxyglucose (FDG), a glucose molecule with a hydroxyl group replaced by radioactive ^{18}F . FDG enters the same metabolic pathways as glucose and is utilized for oncology and brain imaging [1].

Upon injection in the body, the tracer is concentrated in specific tissues, such as a tumor. Positrons emitted from beta decay annihilate with nearby electrons, generating back-to-back 511 keV photons that can be detected by a scintillator crystal coupled to

a photodetector. The location of the annihilation event can be narrowed to a line of response (LOR) from two coincident detections [1]. In PET systems with high timing resolution, the annihilation location can be further constrained to a segment on the LOR. This is known as time-of-flight (TOF) PET, in which high timing resolution results in the reduction of statistical noise. Advantages of TOF PET include faster computer processing times and better image quality [1-2].

Photodetectors and PET

The standard photodetector in clinical PET machines is the photomultiplier tube (PMT). The high gain, fast response and high sensitivity of PMTs have made them a viable detector for PET, but there exist several drawbacks. One, the bulky size of PMTs puts a limit on the spatial resolution of a detector [1]. PMTs are also highly sensitive to magnetic fields. This makes it impossible to implement PET with magnetic resonance imaging (MRI), considered the future of biomedical imaging because of the promise of simultaneous metabolic and anatomical information [3-4].

An area of active research is the study and application of silicon photomultipliers (SiPM). SiPMs are relatively compact and insensitive to magnetic fields while achieving roughly the same gain and sensitivity as PMTs [4-5]. The SiPM is a semiconductor device made up of avalanche photodiode (APD) pixels connected in parallel. Each APD is an individual photon counter and the sum of all the APD pixels is the output of the SiPM. The APDs are operated in Geiger Mode, where the bias voltage applied is greater than the reverse breakdown voltage resulting in a large internal electric field. An incident photon causes a carrier to be injected into this electric field creating a large pulse that can be put into electronics. The specifications of the SiPM vary widely, but for PET applications the greater number of pixels (lower fill factor) is desired because of the high light input to the detector [3,5].

Studies of SiPMs have yielded promising results. Measurements of the inherent coincidence timing resolution using a splitted laser gave timing on the order of 100 ps, suggesting the viability of SiPM for TOF PET [6]. The coincidence timing between two LYSO/SiPM coupled detectors has been measured by Kim et al to be at best 240 ps [7]. However, there are challenges to implementing SiPMs into a full scale PET machine. There is a moderate dependence of gain with bias voltage, so each SiPM would require its own voltage control. Temperature dependence is also an issue. Other challenges exist and are discussed in reference [7], but the potential benefits of SiPM photodetectors for PET make their implementation a promising next step in detector design.

Experiment

Characterization of SiPM

We first wanted to test for ourselves some basic properties of SiPMs. We focus on the 1600 pixel, $25 \mu m^2$ pixel size SiPM (Hamamatsu S10362-025C) because of the large number of photons incident on the photocathode in PET. This sacrifices active area, but it ensures that the photocathode will not be saturated. We will also analyze the properties of the 400 pixel, $50 \mu m^2$ pixel area SiPM (Hamamatsu S10362-050C).

Gain and dark count rate were measured using a single SiPM without an LSO crystal or radioactive source. Detector was kept in black box for both experiments. For gain measurement, SiPM output was amplified using 30 dB preamplifier and signal was read out using a fast oscilloscope (TDC6154, 20 GS/s). Oscilloscope was triggered at 5 mV increments from 5 mV to 50 mV and 1500 events were collected at each trigger level. The result is the energy of the photoelectron (p.e) peaks after gain from both the SiPM and preamp, shown Figure 1. By a linear fit of the amplified energy (charge) of the 1,2,3 and 4 p.e. peaks vs. the unamplified photon energy, the gain of the 1600 pixel SiPM was determined to be $2.0 * 10^5$. Similarly, the gain of the 400 pixel SiPM was found to be $6.2 * 10^5$.

The dark count rate was also measured. The SiPM is a solid-state device with inherent noise due to thermal excitations of the APD pixels, causing uncorrelated photon counts. To make any reliable measurements, it is important to understand and quantify this noise. In order measure the dark count, signal was 'counted' at different levels of noise. The SiPM output was sent to a 10x preamplifier, split and sent to two discriminator inputs. Trigger levels of the discriminator were set to 0.5 p.e. and 1.5 p.e. respectively.

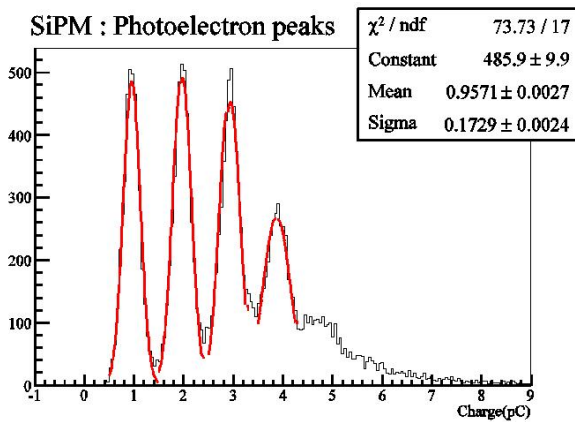


Figure 1: Photoelectron spectrum of SiPM (left peak corresponds to 1 p.e., etc.)

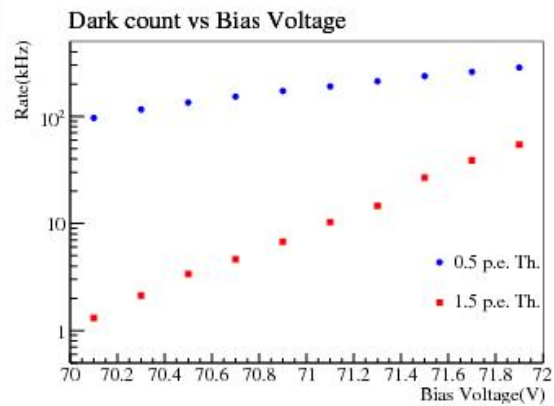


Figure 2: Dark count rate vs. bias voltage, 1600 pixel

These levels varied with applied bias voltage and were set by observing the preamplified pulse in oscilloscope. The discriminated signal was sent to a Lecroy 2551 100 MHz scaler to give a counts per acquisition time for each threshold level. Bias voltage was varied from 70.1 to 71.9 V and the result is shown in Figure 2.

For an operating voltage of 71.0 V, it is clear that the dominant noise is from single photoelectron counts. Although the noise rate is high (~ 110 kHz), the energy is much smaller than a useful PET signal so it is easily filtered. However, if our goal was to count individual photons, the SiPM would not be a good photodetector.

Methods

Two $1 \times 1 \times 10$ mm³ LSO crystals were attached to a pair 1600 or 400 pixel SiPMs using a small amount of fast-drying, transparent epoxy. The crystals were wrapped in teflon tape to keep optical photons internally reflected. Both SiPMs were operated at a bias voltage of 71.0 V. A ²²Na source was used as a positron emitter and placed between the two detectors, as shown in Figure 3.

CAMAC System

A CAMAC data acquisition system with NIM electronics was used to measure coincidence timing and energy resolution.

The SiPM output was put directly in a LeCroy model 612 fast amplifier (10x) and then split using a linear fan-in/fan-out module (LeCroy model 428F). One branch was put in a LeCroy 623B discriminator with a minimum threshold of 30 mV. The discriminated signal was sent to a coincidence unit set to 'AND' logic so as to fire for a coincidence event.

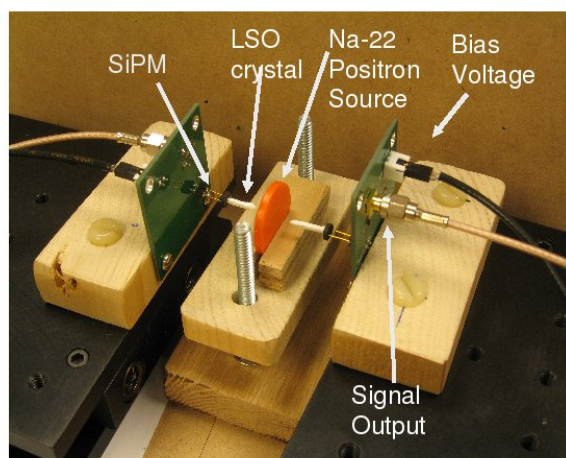


Figure 3: Experimental setup

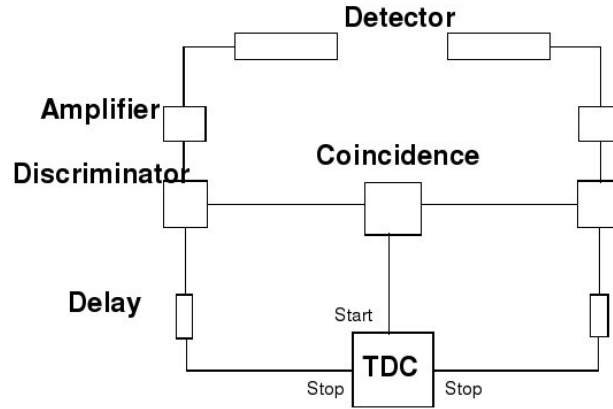


Figure 4: Electronic schematic for coincidence timing measurement using CAMAC system

This output was used for the ADC gate and the TDC start. The other branch of the fan-out module was delayed and sent to the ADC channel inputs for energy information.

To extract timing information, the analog signal was amplified 100x and then put into a discriminator. The discriminator level was set to the lowest possible level above the noise threshold that was observed in oscilloscope. This was necessary to get the best possible timing resolution from our system. Both discriminator outputs were delayed with a 40 ns cable and sent to the stop channels in the TDC for timing information. See Figure 4 for a schematic of the timing electronics.

TDC Calibration

TDC needed to be calibrated to interpret data. Discriminated pulse from a function generator was sent to TDC with 0, 2, 4 ns delays. By measuring TDC values to the delays, conversion factor of 41 ps/bit was obtained.

Fast Oscilloscope

In addition, the coincidence timing and energy resolution were analyzed using a Tektronix DPO7000 series 40 GS/s digital oscilloscope. With the same set-up as in Figure 3, the unamplified SiPM signals were sent to the scope and coincidence events were captured using a logic 'AND' trigger. Each channel was sampled at 20 GS/s and an event was 500 ns, providing 10000 points per saved waveform with a time interval of 0.05 ns between samples.

Results/Analysis

From CAMAC Setup

Results from 1600 pixel SiPM shown in Figure 5. Forty-thousand coincident events in total were collected at a rate of about $\frac{1}{2}$ Hz. The right peak in the charge (energy) spectrum is due to the gamma photon depositing all 511 keV in the scintillator. The left peak is of less energy, in which the gamma has Compton scattered, only depositing a fraction of its energy in the crystal. These events degrade the time resolution and are filtered out for timing measurements. The disparity in relative peak size was most likely due to coupling differences between the SiPM surface and the LSO crystal of the two detectors.

The coincidence timing is presented before (Delta T) and after (Delta T: cut) filtering unwanted events. The timing resolution considering only those events in the 511 keV peak is shown to be 820 ps FWHM. The best energy resolution (from SiPM 1) is 23.9 % FWHM. The discriminator threshold level for timing was set at 50 mV for this timing result. See Figure 6 for timing resolution as a function of varying this threshold.

Temperature sensitivity of the SiPM became apparent during this experiment as ADC spectrum clearly shifted as time progressed. There has been shown to be a considerable gain dependence on temperature in SiPMs [4] and this might be the cause of the spectrum shift. This makes getting good energy resolution at low coincident rates a difficult task!

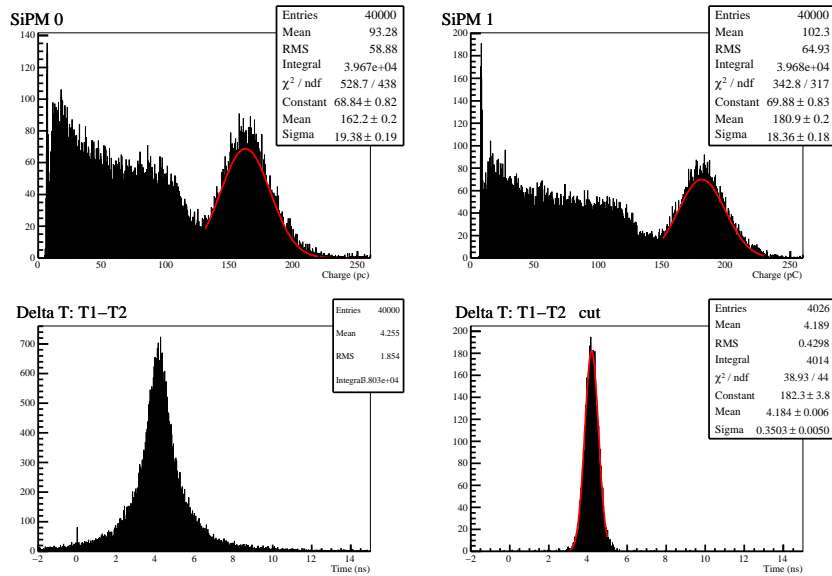


Figure 5: Results: 1600 pixel SiPM, **top:** Energy Spectrum, **bottom:** Coincidence Timing

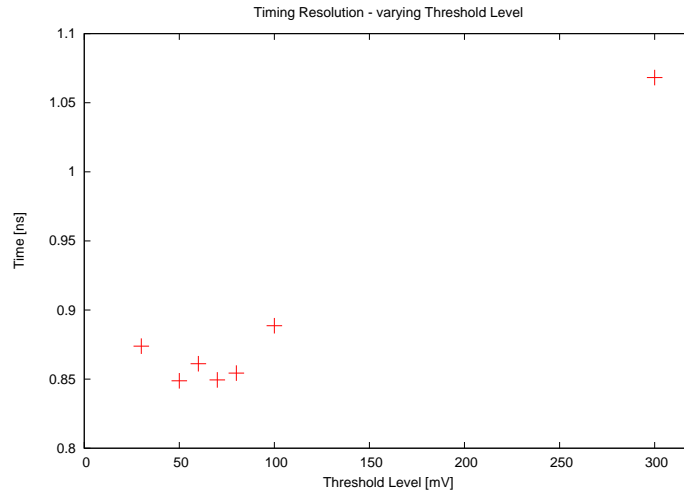


Figure 6: Coincident timing as a function of threshold level

See figures 19 and 20 in the appendix for raw data.

Results from 400 pixel SiPM shown in figure 7. Coincidence timing was 850 ps FWHM and the best energy resolution was 16.4% FWHM.

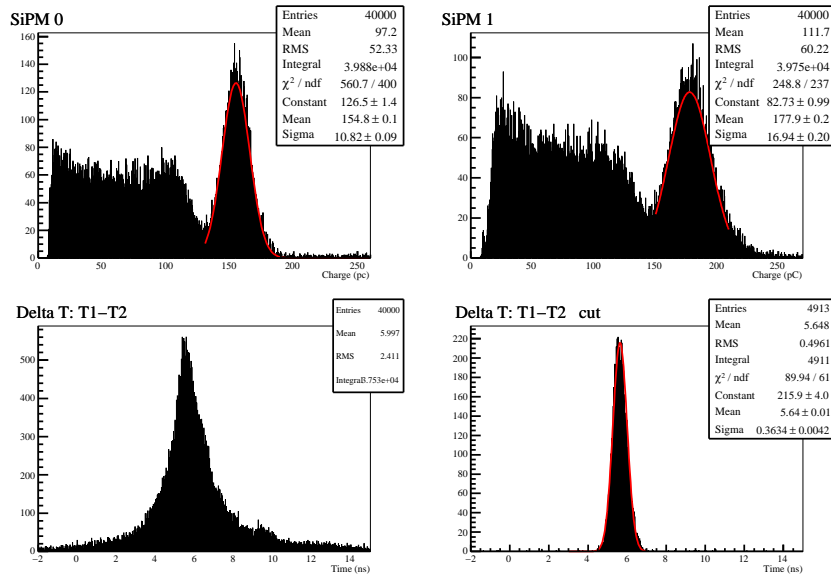


Figure 7: Results: 400 pixel SiPM, **top:** Energy Spectrum, **bottom:** Coincidence Timing

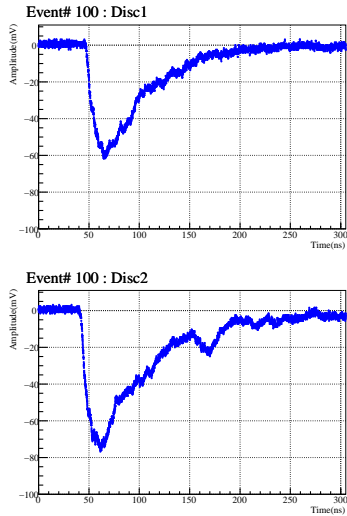


Figure 8: Sample coincident event acquired using digital oscilloscope.

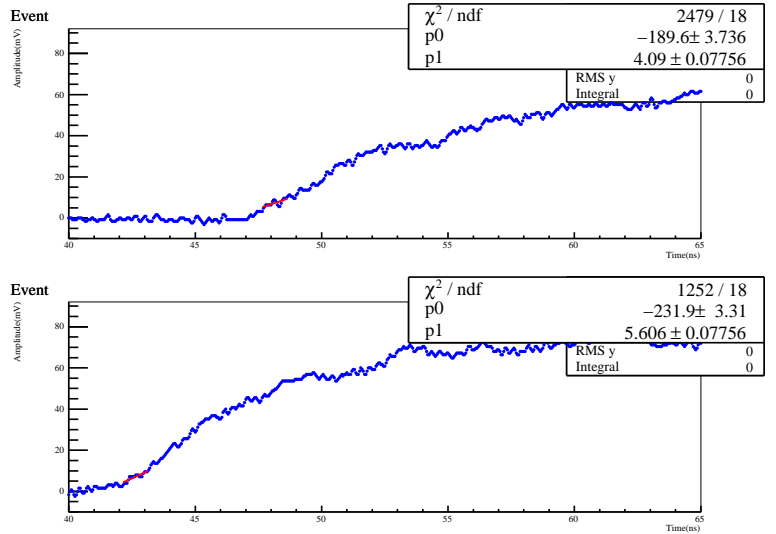


Figure 9: Zoom into rising edge of event in fig 8. Red line is linear fit over n sample points at a specified voltage threshold. Coincidence timing is extracted by examining difference in x-intercept of fits between channels.

From Oscilloscope

Using the 400 pixel SiPMs, 4000 coincidence events in total were collected. Example waveforms from a coincidence event are shown in Figure 8. A linear fit was performed on the rising edge of each waveform at a specified threshold as presented in Figure 9. Coincidence time was found by examining the difference between x-intercept values of the fit between the two channels. The best timing was extracted by fitting to 10 points, corresponding to 500 ps, below threshold level.

Again, by selecting only those events in which all 511 keV of gamma photon energy was deposited, the coincidence timing was found to be 660 ps FWHM. This is shown in Figure 11. The threshold was set to 3 mV for this result, and coincidence timing as a function of fitting threshold is provided in Figure 10. No improvement in time resolution was found for a threshold lower than 3 mV since that was just above the noise level of the signal.

The energy spectrum was determined by integrating discretely under each waveform. The integrated charge was found by implementing the algorithm (from Ohm's Law):

$$\Delta Q = \frac{1}{R} \sum_{i=1}^{N_{\text{sample}}} V[i] \Delta t_i = \frac{\Delta t}{R} \sum_{i=1}^{N_{\text{sample}}} V[i] \quad (1)$$

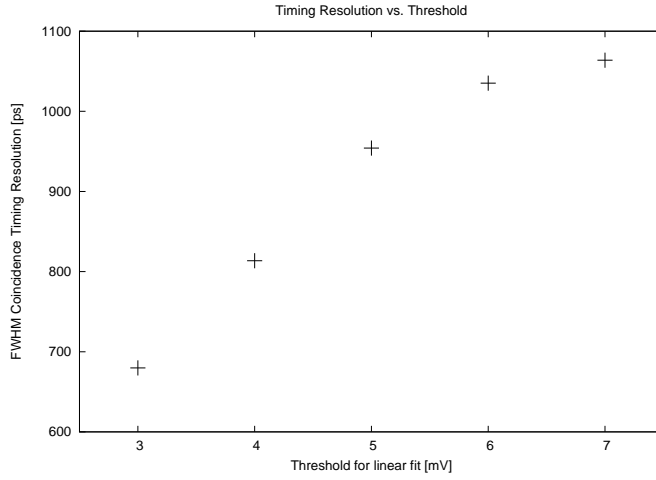


Figure 10: Timing resolution as a function of the linear fit threshold to digitized waveform

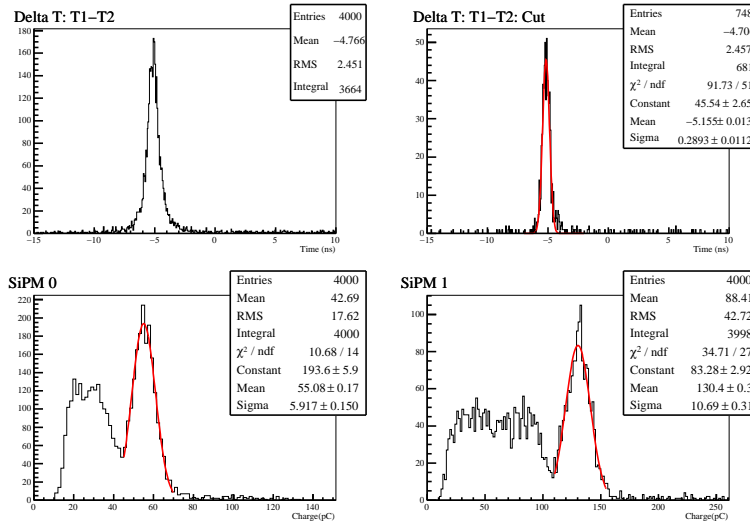


Figure 11: Results from scope: 400 pixel SiPM, **top:** Coincidence Timing, **bottom:** Energy Spectrum

where R is the scope input impedance, Δt , the time interval between sample points, is a constant and $V[i]$ is the signal amplitude at each point. The number of sample points, $NSample$, was 10000 for each event. The energy spectrum is shown in Figure 11. A Gaussian fit to the 511 keV peak gives an energy resolution at best of 19.3% FWHM ¹.

¹Note: SiPM channels 0 and 1 switched between Fig 11 and Fig. 7 when comparing energy spectrum.

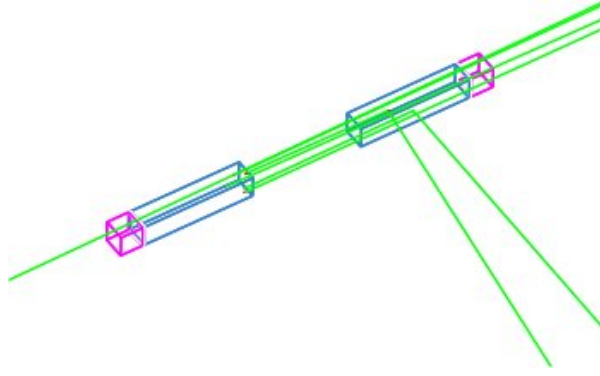


Figure 12: Simulation setup. Green lines indicate gamma path.

Simulation Study

A GEANT4 simulation was created to reproduce the experimental setup presented in Figure 3. The 'world' set-up is shown in Figure 12. Two $1 \times 1 \times 10 \text{ mm}^3$ LSO crystals were attached to a pair of SiPMs and back-to-back 511 keV gamma photons were created directly between the two detectors, labeled 'up' and 'down'. For each event, the gamma trajectory in the crystal was simulated in a stepwise fashion, generating photons by photoelectric or Compton processes. Once produced, each photon was tracked until hitting the detector surface where it was recorded and terminated. The emission spectrum and light yield (30,000 photons/MeV) of LSO was implemented as well.

Five-thousand simulation events were taken in 1000 event intervals. The data was

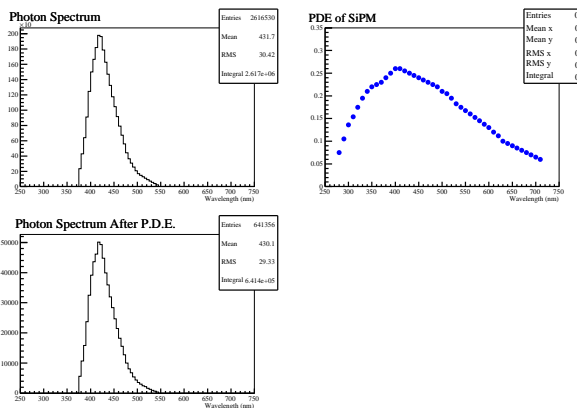


Figure 13: 1600 pixel, **top-right:** Incident photon spectrum, **top-left:** PDE, **bottom:** Photon spectrum after applying PDE

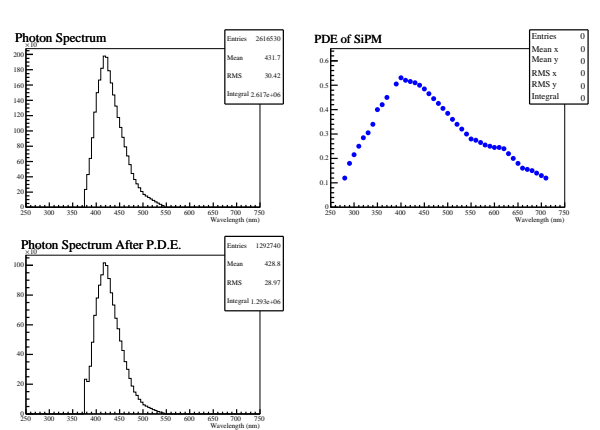


Figure 14: 400 pixel, **top-right:** Incident photon spectrum, **top-left:** PDE, **bottom:** Photon spectrum after applying PDE

analyzed for both 400 and 1600 pixel SiPMs. The number of incident photons at the detector surface is shown in both Figures 15 and 16. It is identical for both SiPMs since the same generated data was used for both. To find the number of fired pixels, we used the expression given by [5]:

$$N_{fired} = N_{pixel} \left(1 - \exp \left(- \frac{N_{photon} * PDE}{N_{pixel}} \right) \right) \quad (2)$$

where N_{photon} is the number of incident photons and the photon detection efficiency

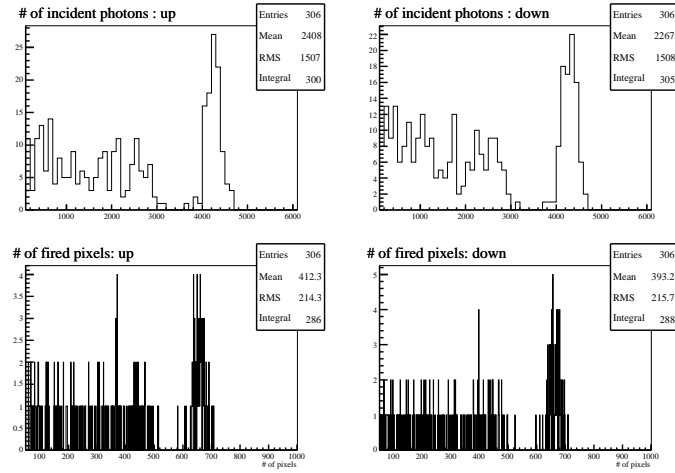


Figure 15: 1600 pixel, **top:** Photons incident on SiPM, **bottom:** Fired pixels

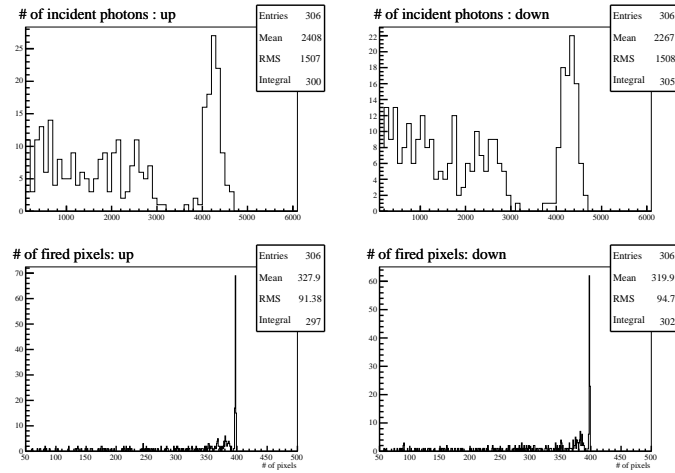


Figure 16: 400 pixel, **top:** Photons incident on SiPM, **bottom:** Fired pixels

(PDE) is provided in [5] and plotted in Figures 13 and 14. Since the photon spectrum and PDE peak at the same energy, the PDE effectively reduces the photon spectrum by a constant factor as shown in Figures 13 and 14. So, in equation (2), PDE was taken to be a constant: 0.2 for 1600 pixel, 0.48 for 400 pixel SiPM.

The number of fired pixels is presented in Figures 15 and 16 for the 1600 pixel and 400 pixel SiPM, respectively. The 400 pixel SiPM shows clear saturation as most of the events cause all 400 pixels to fire. The energy spectrum is directly related to the number of fired pixels and is shown in Figures 17 and 18. A distinction between the Compton and 511 keV peak is clear when using the 1600 pixel SiPM. This is not the case with the 400 pixel SiPM because of saturation.

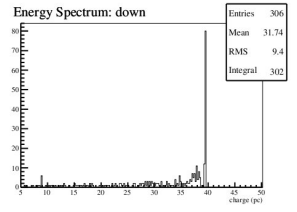
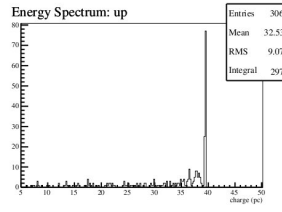
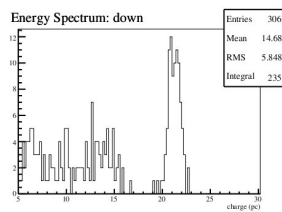
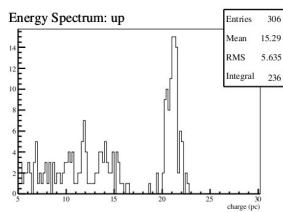


Figure 17: 1600 pixel: Energy spectrum from simulation

Figure 18: 400 pixel: Energy spectrum from simulation, clearly shows signal saturation

Discussion

The best coincidence timing resolution was found to be 660 ps FWHM using waveform sampling. This is good enough for TOF-PET applications. The timing could likely be improved by amplifying the SiPM signal before sending to oscilloscope, allowing for a linear fit to a lower relative threshold level. The best energy resolution, 16.4 % FWHM, was found using the 400 pixel SiPM. The SiPM dark noise was shown to be dominated by low amplitude signals that are easily filtered from a typical PET signal.

Contrary to intuition, it appears the the 400 pixel SiPM would be better suited for PET applications because of its better energy resolution. Because of the large number of incident photons (on the order of thousands), a detector with 400 pixels is expected to be saturated as shown in the simulation data (Figure 18). The experimental results suggest otherwise, the detector does not become saturated. There is a distinct 511 keV peak and events in this peak can be clearly analyzed for timing.

A possible explanation for this is the incorrect assumption that one pixel can detect only one photon. For a 400 pixel SiPM, the duration of a single photoelectron pulse is roughly 30 ns as shown in Figure 21 in the Appendix. An LSO signal, however, has

a width of about 200 ns (see Figure 8). This means that each pixel may fire multiple times during an event, avoiding the saturation predicted by the simulation. In that case, equation (2) can't be applied blindly without considering this effect.

References

- [1] T.K. Lewellen 2008 Recent Developments in PET Detector Technology *Phys. Med. Biol* **53** R287-R317
- [2] W.W. Moses 2007 Recent Advances and Future Advances in TOF PET *Nucl. Instrum. Methods Phys. Res.* **580** 919-924
- [3] W.R. Leo 1994 Techniques for Nuclear and Particle Physics Experiment, 2nd Rev Edition, Springer.
- [4] S. Espana, et al 2008 Performance Evaluation of SiPM Detectors for PET Imaging in the Presence of Magnetic Fields *IEEE* submitted November 14,2008
- [5] Hamamatsu 2008 Multi-Pixel Photon Counter Specification Sheet
- [6] Q. Xie et al 2007 Performance Evaluation of MPPC for PET Imaging *2007 IEEE Nucl. Sci. Symp. Conf. Record* 969-974
- [7] C.L.Kim et al 2008 MPPC for TOF PET Detector and its Challenges *2008 IEEE Nucl. Sci. Symp. Conf. Record* 3586-3590

Acknowledgements

Many thanks to Heejong Kim whose help and guidance were greatly appreciated. He provided the CAMAC acquisition programs, the GEANT4 simulation as well as Figures 1 and 21.

Thanks to the UChicago Electronics Shop for allowing the use of their expensive oscilloscope.

Appendix

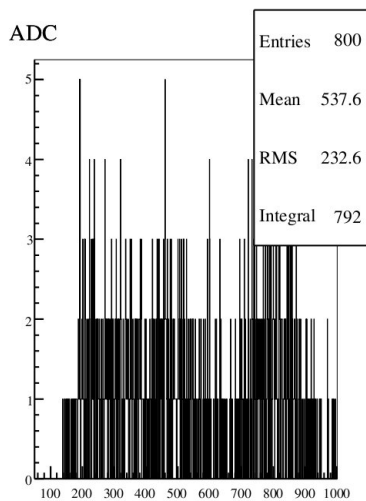


Figure 19: Ch0 ADC spectrum, $t=0$

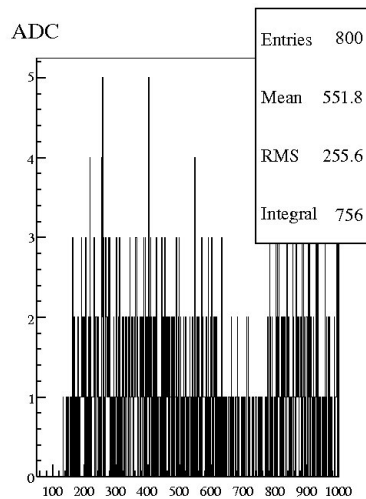


Figure 20: ADC spectrum, $t = 12$ hours later, 511 keV peak shifted off scale

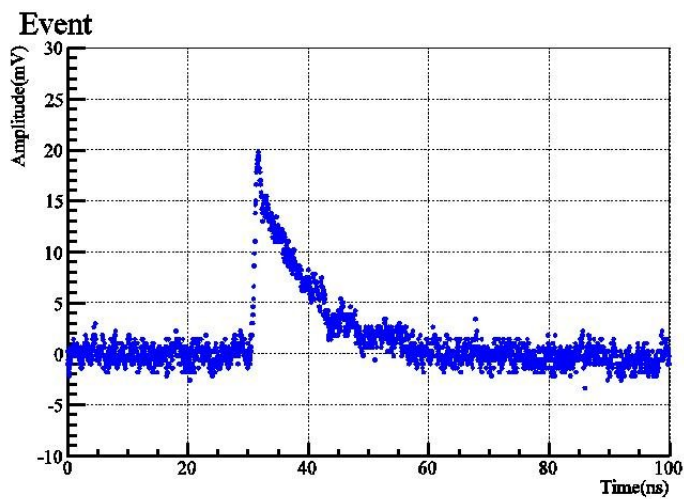


Figure 21: Single photoelectron pulse, 400 pixel SiPM